International Journal of Engineering, Mathematical and Physical Sciences
ISSN: 2517-9934
Vol:11, No:1, 2017

Warning about the Risk of Blood Flow Stagnation after Transcatheter Aortic Valve Implantation

Aymen Laadhari, Gábor Székely

***Abstract*—**In this work, the hemodynamics in the sinuses of Valsalva after Transcatheter Aortic Valve Implantation is numerically examined. We focus on the physical results in the two-dimensional case. We use a finite element methodology based on a Lagrange multiplier technique that enables to couple the dynamics of blood flow and the leaflets' movement. A massively parallel implementation of a monolithic and fully implicit solver allows more accuracy and significant computational savings. The elastic properties of the aortic valve are disregarded, and the numerical computations are performed under physiologically correct pressure loads. Computational results depict that blood flow may be subject to stagnation in the lower domain of the sinuses of Valsalva after Transcatheter Aortic Valve Implantation.

***Keywords*—**Hemodynamics, Transcatheter Aortic Valve Implantation, blood flow stagnation, numerical simulations.

I. Introduction

THIS framework concerns the numerical modeling of hemodynamics in the sinuses of Valsalva coupled with the movement of the aortic valve after Transcatheter Aortic Valve Implantation. The heart is the central pumping organ of the cardiac function which is of extreme complexity covering widely different spatio-temporal scales. The heart is composed by four chambers and four valves at the corresponding chamber openings which allow blood to flow in the right directions. In particular, the aortic valve is the gateway for oxygenated blood from the heart to the rest of the body. Natural aortic valve consists of three symmetric leaflets of similar size, faced by three corresponding pouches of the aorta called sinuses of Valsalva, see Fig. 1. The physiological function of the aortic valve can be summarized as follows: the leaflets synchronize the opening during systole and the closing during diastole, leading to correct blood ejection and preventing regurgitation. Many are the pathological cases where the aortic valve is dysfunctional such as stenosis and regurgitation. In particular, the aortic stenosis represents an abnormal narrowing of the aortic valve which prevents the full opening during the systolic phase. Nowadays, heart disease represents one of the major health problems, and the aortic stenosis is considered to be the most important disorder in valve diseases. It affects 3% of persons older than 65 years [19] and more than 14% of individuals over 75 years [14], leading very often to heart failure. In the United States, approximately 1.5 million adults suffer from the aortic stenosis, while 33% of them suffer from a severe stenosis, see [3]. The calcified aortic valve represents the most prevalent valve disease among the elderly [5], so that valve replacement is the only effective therapy. The surgical aortic valve replacement is the conventional treatment for such diseased valves. That consists in dissecting the diseased valve, cleaning the surrounding region and suturing a new bioprosthetic or mechanical valve. However, a large number of patients are not eligible for an open heart surgery, such as elderly with high risk of operative mortality and younger patients who remain inoperable until older ages to avoid multiple invasive surgeries (because of the low sustainability of the surgical aortic valve replacement technique).

As a promising alternative, the Transcatheter Aortic Valve Implantation, referred to as TAVI, represents a new and revolutionary therapy in the field of cardiothoracic surgery with more than 100.000 implantations performed worldwide [18]. This less invasive alternative enables the valve replacement without performing an open-heart surgery. It consists in delivering a prosthetic valve mounted on a catheter guided stent into a calcified native valve. In general, the native diseased leaflets are heavily calcified and play the role of rigid walls, which are fixed by the stent between the implanted valve and the aortic wall [6]. Several postoperative complications after TAVI have been reported in the literature such as: the paravalvular regurgitation affecting up to 70% of patients after TAVI [23], malpositioning, late migration, or blocking coronary ostia [15]. A recent review of the most relevant complications post-TAVI is available in [15]. In such situations, corrective measures (e.g. valve-in-valve implantation, post-dilation, snare repositioning) or emergency open heart surgery are required [15].

A growing literature has been devoted to the experimental research in the field of Transcatheter Aortic Valve Implantation. However, a little progress has been reported at the numerical level. The numerical investigation of the hemodynamics after TAVI can certainly be of great potential in the improvement of this technology and the enhancement of patients life quality.

In the present work, we study the incidence of blood stagnation after TAVI in the two-dimensional case. Blood stagnation corresponds to the zones of low velocities and can represent an evaluating criterion of the TAVI efficiency. Clinically, they are considered as a source for increased probability of thrombosis (clotting) and embolism (if a clot is detached and travels through the cardiovascular system). This

A. Laadhari is with the Department of Information Technology and Electrical Engineering, Swiss Federal Institute of Technology Zürich (Eidgenössische Technische Hochschule Zürich), CH-8092 Zürich, Switzerland (e-mail: laadhari@vision.ee.ethz.ch).

G. Székely is with the Department of Information Technology and Electrical Engineering, Swiss Federal Institute of Technology Zürich (Eidgenössische Technische Hochschule Zürich), CH-8092 Zürich, Switzerland.

Fig. 1 Different views of the aortic valve with realistic shapes in the fully closed configuration

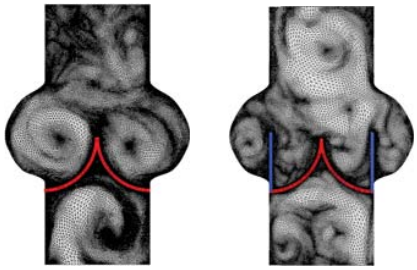

Fig. 2 A sketch for the computational domains and corresponding finite element network in 2D. Left: healthy aortic valve (red). Right: TAVI with implanted (red) and calcified (blue) leaflets

dangerous situation can trigger stroke if a clot travels to the head, or heart attack if it travels to the coronary arteries. For patients having mechanical heart valves, blood flow stagnation represents a well-known problem resulting from the high shear stress induced by the valve design [28]. The main objective in this numerical study is to analyse the incidence of blood stagnation after TAVI in the two-dimensional case while taking into consideration the presence of the calcified native (diseased) leaflets. Our numerical study reveals that this setting produce substantial modifications in the blood flow pattern and can promote blood stagnation in the sinuses.

Section II briefly describes the mathematical formulation of the coupled nonlinear problem describing the dynamics of blood flow and valve. Section III provides a set of numerical examples showing the blood flow patterns in the healthy case and highlighting the main changes after Transcatheter Aortic Valve Implantation. We close with some comments about the forthcoming extensions in Section IV.

II. Mathematical setting

The computational domain is made up of the left ventricular outflow tract, the sinuses of Valsalva and the ascending aorta. We reproduce the same geometry used in [4], [10]. The two-dimensional computations enable to qualitatively study the basic fluidic phenomena at an affordable computational burden. We briefly describe the mathematical model and we rather focus on the physical results, while a detailed description of the numerical aproach will be provided in [9].

Let $d = 2$ design the space dimension and $T > 0$ represent the period of the computations. For any time $t \in (0, T)$, the exterior of the domain occupied by the set of moving leaflets $\Gamma_i(t)$ and calcified leaflets S_i is denoted as $\Omega(t)$ (depending on t due to the valve motion), with $i \in [1, \mathrm{d}]$. The diseased leaflets S_i are assumed symmetric and behave as a rigid walls. Regarding the blood flow interaction with the leaflets, the no slip condition is assumed on the surface of the leaflets. Accordingly, a moving boundary condition for the blood velocity $\boldsymbol{u}$ holds on the leaflets. Let $\boldsymbol{u}_i^\star$ stand for the corresponding cusp velocity on $\Gamma_i(t) \cup S_i$ with $i \in [1, \mathrm{d}]$. Since the calcified leaflets S_i behave stiff, we assume $\boldsymbol{u}_i^\star = \mathbf{0}, \forall i \in [1, \mathrm{d}]$. Regarding the moving leaflets Γ_i, only the normal component of the leaflets velocity has a contribution to its motion.

The fluid Cauchy stress tensor is given by

$$\boldsymbol{\sigma}(\boldsymbol{u}, p) = 2\mu \mathbf{D}(\boldsymbol{u}) - \mathrm{p}\boldsymbol{I},$$

where $\mathbf{D}(\boldsymbol{u}) = \left(\nabla \boldsymbol{u} + \nabla \boldsymbol{u}^T\right)/2$ and $\boldsymbol{I}$ represent the strain and identity tensors, respectively. Fully developed turbulence is rarely observed in healthy humans [13], and the laminar behavior of blood can be assumed on large vasculature [2]. Blood flow is assumed homogeneous, incompressible and Newtonian. Therefore, the velocity, pressure and the blood/leaflets traction $\boldsymbol{\lambda}$ obey the conservation equations for mass and momentum:

$$\rho\left(\frac{\partial \boldsymbol{u}}{dt} + \boldsymbol{u} \cdot \nabla \boldsymbol{u}\right) - \mathbf{div}\, \boldsymbol{\sigma}(\boldsymbol{u}, \mathrm{p}) + \sum_{i \in [1,\mathrm{d}]} (\delta_{\Gamma_i} + \delta_{S_i})\, \boldsymbol{\lambda} = \mathbf{0}, \quad \text{in } (0,T) \times \Omega, \tag{1}$$

$$\operatorname{div} \boldsymbol{u} = 0, \quad \text{in } (0,T) \times \Omega, \tag{2}$$

$$\left[\boldsymbol{\sigma}\mathbf{n}\right]_-^+ = -\boldsymbol{\lambda}, \quad \text{in } (0,T) \times \Gamma_i(t) \cup S_i, \tag{3}$$

$$[\boldsymbol{u}]_-^+ = \mathbf{0}, \quad \text{in } (0,T) \times \Gamma_i(t) \cup S_i. \tag{4}$$

where the Dirac measure δ allows to localise the leaflets. The Lagrange multiplier $\boldsymbol{\lambda}$ enforces locally the constraint (4) and enables to calibrate the normal stress discontinuities across the leaflets (3). We assume constant density $\rho = 1.06\, g/cm^3$ and dynamic viscosity $\mu = 0.035\, g/cm/s$ for blood flow. The aortic wall is assumed rigid. This limitation is not too severe and reflects the case of elderly patients with severe aortic stenosis and undergoing a Transcatheter Aortic Valve Implantation, for which the aorta behaves almost like a rigid wall [24]. Pulsatile pressure pulses are imposed on both the left-ventricle P_{LV} and the ascending aorta P_{Ao} by prescribing the normal component of the normal stresses:

$$\boldsymbol{\sigma}\mathbf{n} = -P_{\mathrm{LV/Ao}}(t)\mathbf{n}.$$

A periodic left-ventricular pressure waveform $P_{\mathrm{LV}}(t)$ drives the flow through the model. To prescribe the downstream systemic circulation, we consider a geometrical multiscale model consisting of the three-element Windkessel model, see Fig. 3. This model allows to mimic the physiological pressure pulse [25]. It accounts for the arterial compliance and blood viscosity through a capacitor C, a peripheral resistance R_P and a systemic resistance R_D, suitably adjusted. The volumetric flow rate $Q(t)$ is given by the fluid problem, while the stored pressure $P^*(t)$ is computed dynamically. The reduced-order model reads:

$$P_{\mathrm{Ao}}(t) + CR_D \frac{dP_{\mathrm{Ao}}(t)}{dt} = \left(R_P + R_D\right)Q(t) + CR_PR_D \frac{dQ(t)}{dt}, \quad t \in (0,T).$$

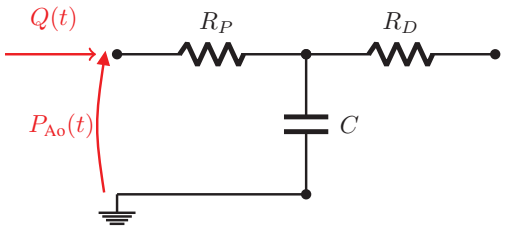

Fig. 3 Schematic representation of a three-element Windkessel model used to set the boundary conditions on the outlet

Regarding the geometrical description of the leaflets, a fully Eulerian framework is considered and we use an implicit representation, see [10]. Very briefly, $\forall i \in [0, \mathrm{d}]$, each leaflet $\Gamma_i(t)$ or S_i is described using two level set embedding functions φ_i and ψ_i such that

$$\Gamma_i(t) = \Big\{ \boldsymbol{x}(t) \in \Omega(t) : \varphi_i(t; \boldsymbol{x}) = 0 \text{ and } \psi_i(t; \boldsymbol{x}) \leqslant 0 \Big\}.$$

We usually introduce φ_i, $i \in [0, \mathrm{d}]$, as signed distance functions. In practice, we need some experimental measurements of the leaflets' dimensions at both open and closed positions. Some descriptors are subsequently introduced in order to build the realistic geometrical shapes of the leaflets, see Fig. 1. A second-order algebraic surface [9], [10] allows to fit the valvular geometry:

$$\varphi_i(t; x, y) = \sum_{j+k \leqslant 2} \alpha_{jk}(t)\, x^j y^k, \quad \forall (x, y) \in \Omega(t),\ i \in [0, \mathrm{d}].$$

In such an Eulerian framework, a regularization approach is commonly introduced to avoid using meshes that fit the movement of the valve, see e.g. [11], [12]. Let us introduce a regularization parameter ε proportional to the mesh size h. The Dirac measure δ is regularized in a banded strip of width 2ε around the leaflets, and the regularized function is given by:

$$\delta_\varepsilon(\varphi) = \begin{cases} 0, & \text{if } \varphi < -\varepsilon \\ \dfrac{1}{2\varepsilon}\left(1 + \cos\left(\dfrac{\pi\varphi}{\varepsilon}\right)\right), & \text{when } |\varphi| \leqslant \varepsilon, \\ 0, & \text{if } \varphi > \varepsilon. \end{cases}$$

For any given function $\zeta(\cdot)$ defined on a surface Γ, an extension $\tilde{\zeta}(\cdot)$ to Ω is required, and the surface integrals are approximated by:

$$\int_\Gamma \zeta(\boldsymbol{x})\, d\boldsymbol{s} = \int_\Omega |\nabla\varphi|\, \delta_\Gamma\, \tilde{\zeta}(\boldsymbol{x})\, d\boldsymbol{x} \approx \int_\Omega |\nabla\varphi|\, \delta_\varepsilon(\varphi)\, \tilde{\zeta}(\boldsymbol{x})\, d\boldsymbol{x}.$$

Let θ stand for the leaflet aperture angle, and it varys between the minimum opening angle $\theta_m = 5$ degrees and the maximum opening angle $\theta_M = 75$ degrees in the healthy case. A geometrical multiscale coupling model enables to follow the leaflets movement described through the aperture angle θ. To circumvent numerical issues related to the large deformations and fast movement of the leaflets, Korakianitis et al. [8] introduced a lumped model, based on several experimental and clinical observations, that describes the movement of the leaflets in terms of the angle θ. Very briefly, it summarizes the angular momentum balance in the aortic valve, while considering the friction from neighboring tissue resistance, transvalvular pressure gradient ΔP, dynamic motion of blood acting on the leaflets, and the influence of downstream vortices. The model reads:

$$\frac{d^2\theta}{dt^2} + \Psi_f \frac{d\theta}{dt} = \Psi_p \Delta P \cos\theta + \Psi_q Q \cos\theta + \chi \Psi_v Q \sin 2\theta$$

where $\chi = \max(\Delta P, 0)/\Delta P$, $\Psi_p = 4.125\, rad\, cm^2/s^2/dyn$, $\Psi_v = 7 rad/s/cm^3$, $\Psi_f = 50 s^{-1}$ and $\Psi_q = 2 rad/s/cm^3$ are the model parameters. This model was validated, as it provided comparable numerical results to those illustrated in some medical textbooks [8].

This model has been reformulated in terms of a variational formulation and has been implemented from scratch in a finite element framework. A monolithic approach combined with a fully implicit scheme ensures the best stability and efficiency especially for relatively large Reynolds numbers around the systolic peak.

The present method has been implemented using the C++ library for scientific computing Rheolef [21]. Distributed-memory parallelism relies on MPI [16], and parallel computations were performed on the BIWI cluster machines at the Swiss Federal Institute of Technology Zürich. The package Mumps [1], [17] is used for the factorization and as direct solver on distributed memory architectures. Results are displayed graphically using the softwares Paraview [20] and Gnuplot [27].

This work is part of a larger, ongoing project to model the dynamics of heart valves. A detailed description of the mathematical setting, numerical issues and model validation is published elsewhere [9], while we only focus here on some qualitative physical results in the two-dimensional case.

III. Results and Discussion

A. Healthy Aortic Valve in the Two-Dimensional Case

In this example, we test the aforementioned model in the two dimensional case with a healthy aortic valve. The discretized fluid domain has $26'578$ mesh elements and is built using the mesh generator Gmsh [7]. We choose a time step size equal to 5×10^{-3} s. We prescribe a periodic left ventricular pressure at the upstream boundary, while we run the simulation over several heart beats until obtaining a fully periodic pressure at the downstream boundary. The parameters of the three-element Windkessel model are given by: $R_P = 168\, dyn\, s\, cm^{-5}$, $R_D = 2382\, dyn\, s\, cm^{-5}$ and $C = 9.45 \times 10^{-4}\, cm^5 dyn^{-1}$. The fully periodic regime is achieved after almost five or six heartbeats. The movement of the leaflets is given by solving the reduced-order model at each time step.

During the sixth cardiac cycle, the peak systole is approximately reached at $t = 4.434$ s, in which the leaflets are completely open and the jet is fully developed. The maximum velocity is around $256\, cm\, s^{-1}$. The leaflets close when the valve is subjected to a flow reversal in the opposite direction to its opening. During the deceleration phase, the pressure gradient between the the aorta and left ventricle rapidly decreases and leads to the valve closure. The fast movement of the leaflets moves backward blood flow into the

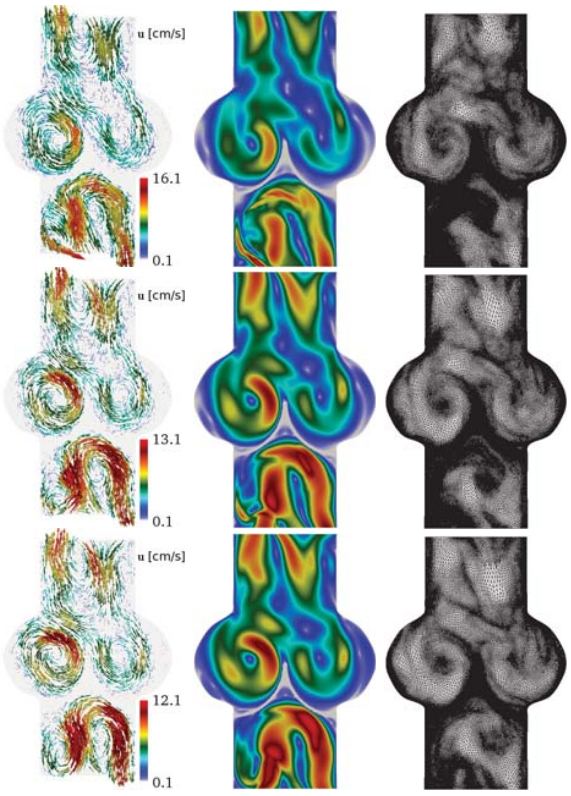

Fig. 4 Snapshots showing the blood flow patterns in the vicinity of a healthy valve and the corresponding adapted meshes at successive times $t \in \{5.209, 5.379, 5.516\}$, respectively from top to bottom. The gray color corresponds to $\|u\| < 0.1\, cm/s$

sinuses of Valsalva. Consequently, a vortical flow pattern is developed in the sinuses.

In Fig. 4 we report some snapshots showing the velocity profiles and the corresponding meshes at particular times during the diastolic phase. The numerical results correspond to the sixth cardiac cycle when a fully periodic regime is established. In particular, we observe a very low velocity in the vicinity of the leaflets.

B. Blood Stagnation after Transcatheter Aortic Valve Implantation

We thereafter undertook a numerical investigation to assess the implications of Transcatheter Aortic Valve Implantation in the sinuses of Valsalva. We assume that the calcified native leaflets behave as a rigid wall. We perform simulations in the two-dimensional case until reaching a fully periodic regime. In this work, we assume that the stagnation zones are the dead zones characterized by low velocity magnitude, below a threshold value $\|\boldsymbol{u}\| < 0.1\, cm/s$. Notice that blood flow stagnates in these zones and may coagulate in a threshold-like manner [26]. A more sophisticated criterion of thrombosis potential based on the computation of the shear rate [22] will be investigated in [9]. Snapshots in Fig. 5 clearly show that some stagnant regions (gray-colored) of low flow $\left(\|\boldsymbol{u}\| < 0.1 cm/s\right)$ are created after Transcatheter Aortic

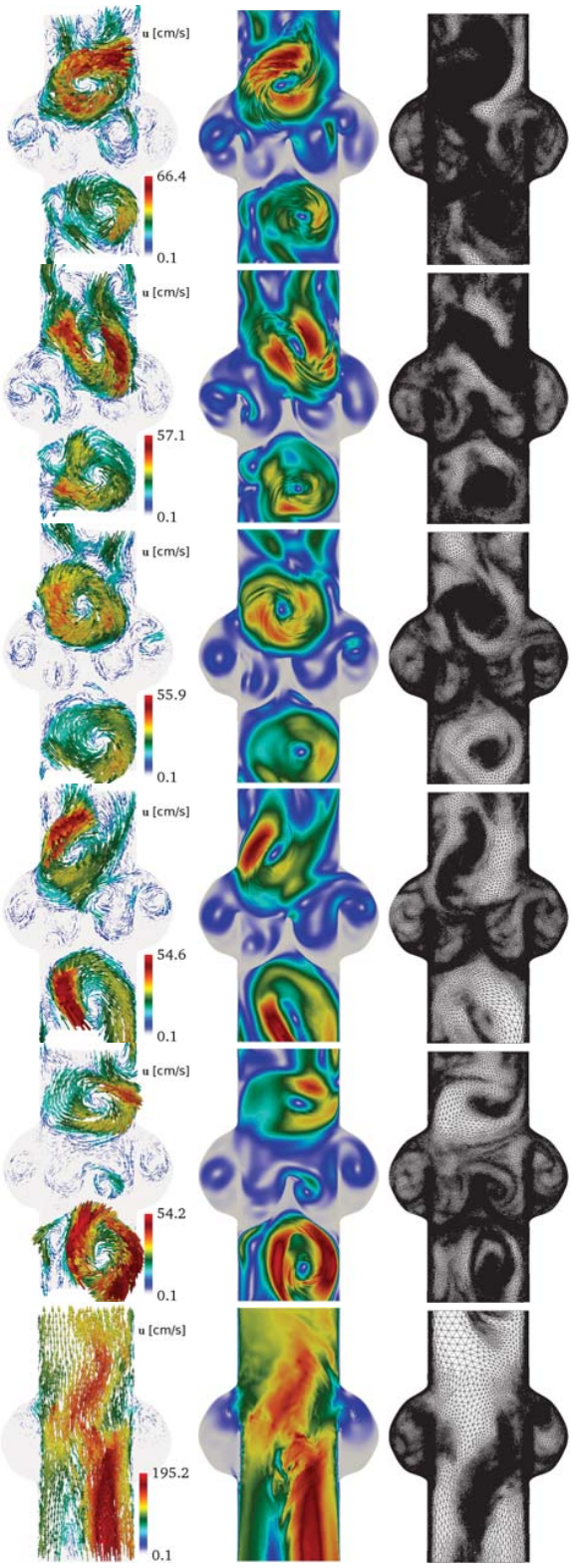

Fig. 5 Snapshots showing the blood flow patterns and corresponding adapted meshes at successive times $t \in \{5.378, 5.428, 5.499, 5.558, 5.621, 5.657\}$, respectively from top to bottom. The gray color corresponds to the stagnation areas for $\|u\| < 0.1\, cm/s$

Valve Implantation in the bottom of the sinuses of Valsalva. However, the numerical results in the healthy case do not show such dead zones, see Fig. 4.

Our understanding is as follows. In the case of healthy leaflets, the valve closure at early diastole is very fast due to the reversal flow. Accordingly, the blood flow is strongly pushed in the sinuses of Valsalva. During the systolic phase, a continuous recirculation of blood in the sinuses is observed. However, after Transcatheter Aortic Valve Implantation, the calcified leaflets can represent an obstruction preventing blood to be correctly pushed in the sinuses. The blood flow patterns is then significantly modified after Transcatheter Aortic Valve Implantation, and the diseased leaflets prevents the full recirculation of blood in the sinuses, see Fig. 5.

IV. Concluding Remarks

In this conference paper, we have used an Eulerian finite element method for the numerical modeling of hemodynamics in the sinuses of Valsalva in the presence of the aortic valve. The mechanical properties of the leaflets have been disregarded. The numerical method is based on the use of the standard Newton method and a monolithic fluid solver has been implemented. The numerical results in the two-dimensional case highlight a potential thromboembolic complication in the sinuses of Valsalva after Transcatheter Aortic Valve Implantation. Further investigations of this work are currently ongoing. In particular, we are investigating a quantification of the extent of the stagnation areas using more accurate criteria in both two-dimensional and three-dimensional cases.

Acknowledgment

The authors gratefully acknowledge the financial support by the Swiss National Science Foundation through the grant **320030-149567**.

References

[1] P. R. Amestoy and I. S. Duff and J. Koster and J.-Y. L'Excellent, *A Fully Asynchronous Multifrontal Solver Using Distributed Dynamic Scheduling*, SIAM J. Matrix Anal. Appl., 2001, 23(1):15-41.

[2] M. Astorino, J. Hamers, S. C. Shadden and J.-F. Gerbeau, *A robust and efficient valve model based on resistive immersed surfaces*, Int. J. Numer. Methods Biomed. Engrg. **28(9)**:937–959 (2012).

[3] D. S. Bach, *Prevalence and Characteristics of Unoperated Patients with Severe Aortic Stenosis*, J. Heart Valve Dis. 2011;20:284-291.

[4] S. Chandra, N. M. Rajamannan and P. Sucosky, *Computational assessment of bicuspid aortic valve wall-shear stress: implications for calcific aortic valve disease*, J. Biomechanics and Modeling in Mechanobiology 2012, **11(7)**:1085-1096.

[5] E. De Marchena, J. Mesa, S. Pomenti, C. M. Kall, X. Marincic, K. Yahagi, E. Ladich, R. Kutys, Y. Aga, M. Ragosta, A. Chawla, M. E. Ring and R. Virmani, *Thrombus Formation Following Transcatheter Aortic Valve Replacement*, JACC: Cardiovascular Interventions 2015, 8(5):728-739

[6] R. V. Freeman and C. M. Otto, *Spectrum of calcific aortic valve disease. Pathogenesis, disease progression and treatment strategies*, Circulation. 2015, 111:3316-3326.

[7] C. Geuzaine and J.-F. Remacle, *Gmsh: A 3-D finite element mesh generator with built-in pre- and post-processing facilities*, Int. J. Numer. Meth. Engng., 2009, 79: 1309-1331.

[8] T. Korakianitis and Y. Shi, *A concentrated parameter model for the human cardiovascular system including heart valve dynamics and atrioventricular interaction*, Med. Eng. Phys. 2006, 28(7):613-628.

[9] A. Laadhari and G. Székely, *Eulerian finite element method for the numerical modeling of fluid dynamics of natural and pathological aortic valves*, J. Comput. Appl. Math. (submitted 2016).

[10] A. Laadhari, A. Quarteroni, *Numerical modeling of heart valves using resistive Eulerian surfaces*, Int. J. Numer. Method. Biomed. Eng. 32(5) (2016).

[11] A. Laadhari, P. Saramito, C. Misbah, *An adaptive finite element method for the modeling of the equilibrium of red blood cells*, Int. J. Numer. Meth. Fluids 80 (2016) 397–428.

[12] A. Laadhari, P. Saramito and C. Misbah, *Computing the dynamics of biomembranes by combining conservative level set and adaptive finite element methods*, J. Comput. Phys. 263 (2014) 328–352.

[13] J. K-J. Li, *Laminar and turbulent flow in the mammalian aorta: Reynolds number*, Journal of Theoretical Biology (1988), **135(3)**:409–414.

[14] M. Lindroos, M. Kupari, J. Heikkilä, R. Tilvis, *Prevalence of aortic valve abnormalities in the elderly: an echocardiographic study of a random population sample*, J. Am. Coll. Cardiol. 1993;21(5):1220-1225.

[15] S. N. Miandoab and R. E. Michler, *A Review of Most Relevant Complications of Transcatheter Aortic Valve Implantation*, ISRN Cardiology 2013;12:2013.

[16] M.P.I. Forum, *MPI: A Message-Passing Interface Standard*, http://www.mpi-forum.org (Accessed: 28.11.2016).

[17] MUMPS: MUltifrontal Massively Parallel Solver, http://mumps.enseeiht.fr/index.php (Accessed: 28.11.2016).

[18] J. D. Newton, S. Redwood and B. D. Prendergast, Transcatheter aortic valve implantation: a durable treatment option in aortic stenosis?, Heart 2015, 101(12):913-914.

[19] C. M. Otto, J. Knuusisto, D. D. Reichenbach, A. M. Gown and K. D. O'Brien, *Characterization of the early lesion of "degenerative" valvular aortic stenosis. Histological and immunohistochemical studies*, Circulation. 1994;90(2):844-853.

[20] Paraview: Parallel visualization application, http://paraview.org (Accessed: 28.11.2016).

[21] P. Saramito, *Efficient C++ finite element computing with Rheolef*, CNRS-CCSD ed., 2013. http://www-ljk.imag.fr/membres/Pierre.Saramito/rheolef/rheolef-refman.pdf (Accessed: 22.09.16).

[22] K. S. Sakariassen, S. R. Hanson and Y. Cadroy, *Methods and models to evaluate shear-dependent and surface reactivity-dependent antithrombotic efficacy*, Thromb Res. 2001; 104: 149-174.

[23] J. M. Sinning, M. Vasa-Nicotera, D. Chin, C. Hammerstingl, A. Ghanem, J. Bence, J. Kovac, E. Grube, G. Nickenig and N. Werner *Evaluation and management of paravalvular aortic regurgitation after transcatheter aortic valve replacement*, J. Am. Coll. Cardiol. 2013,62:11-20.

[24] B. A. Towfiq, J. Weir and J.M. Rawles, *Effect of age and blood pressure on aortic size and stroke distance*, British Heart J. 1986, **55(6)**:560-568.

[25] N. Westerhof, G. Elzinga and P. Sipkema, *An artificial arterial system for pumping hearts*, J. Appl. Physiol. 1971, **31(5)**, 776-781.

[26] H. J. Weiss, V. T. Turitto and H. R. Baumgartner, *Role of shear rate and platelets in promoting fibrin formation on rabbit subendothelium - studies utilizing patients with quantitative and qualitative platelet defects*, J. Clin. Invest. 1986; 78: 1072-1082.

[27] T. Williams and C. Kelley, *Gnuplot: An Interactive Plotting Program* http://www.gnuplot.info (Accessed: 28.11.2016).

[28] Y. R. Woo and A. P. Yogananthan, *In vitro pulsatile flow velocity and shear stress measurements in the vicinity of mechanical mitral heart prostheses*, J. Biomech. 1986;19:39-51.